Volume 54 | Number 91 | 25 November 2018 | Pages 12777–12894

ChemComm

Chemical Communications

rsc.li/chemcomm

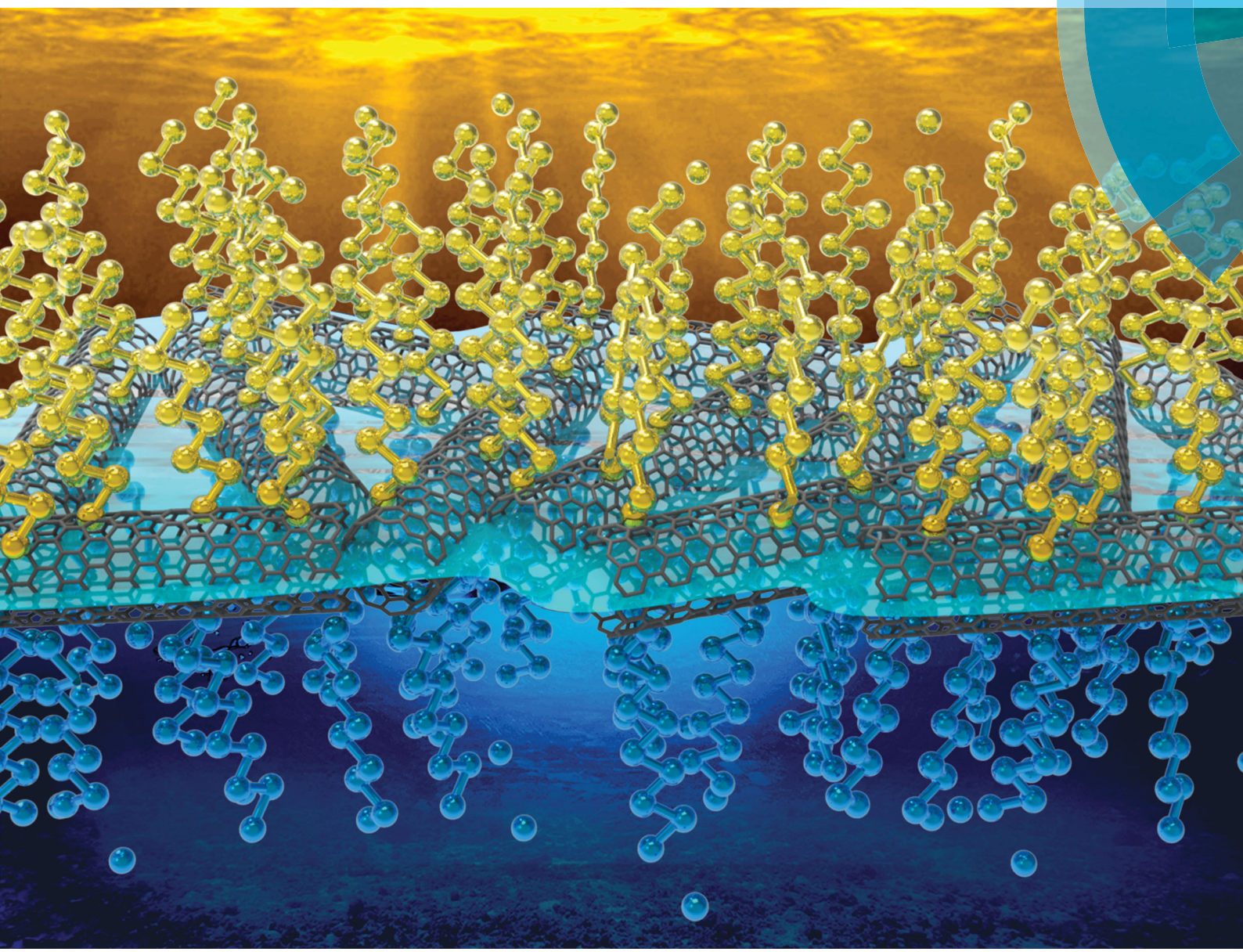

ISSN 1359-7345

ROYAL SOCIETY OF CHEMISTRY

COMMUNICATION

Peng Xiao, Youju Huang, Tao Chen *et al.*

A lotus-inspired janus hybrid film enabled by interfacial self-assembly and *in situ* asymmetric modification

ChemComm

COMMUNICATION

View Article Online
View Journal | View Issue

Cite this: *Chem. Commun.*, 2018, **54**, 12804

Received 3rd September 2018,
Accepted 27th September 2018

DOI: 10.1039/c8cc07143h

rsc.li/chemcomm

A lotus-inspired janus hybrid film enabled by interfacial self-assembly and *in situ* asymmetric modification†

Yun Liang,[ab] Jiangwei Shi,[a] Peng Xiao,[ab]* Jiang He,[ab] Feng Ni,[ab] Jiawei Zhang,[ab] Youju Huang,[ab]* Chih-Feng Huang[c] and Tao Chen[ab]*

A lotus leaf inspired Janus hybrid film was exquisitely fabricated through a self-assembly process at the air/water interface with subsequent *in situ* asymmetric modification at the oil/water interface. The interfacial asymmetric decoration strategy thus provides a novel pathway for achieving a 2D Janus hybrid film with asymmetric wettability and functionality.

Janus materials that integrate asymmetric chemistry or morphology into one surface have attracted tremendous attention due to their significant and fascinating performances in the academic and industrial fields.[1–5] Such specifically anisotropic structures can emerge as different forms, such as zero dimensional (0D) particles,[6–9] one dimensional (1D) cylinders or fibres[10–13] and two-dimensional (2D) sheets, discs or films.[2,14–18] In particular, owing to the unique physical, chemical and electrical properties, 2D Janus films have blossomed in recent years. Although massive efforts have been dedicated to constructing Janus films, a cost-effective, efficient and scalable approach is eagerly sought. One recent example is the direct multilevel self-assembly of azopyridine derivatives and poly(acrylic acid) for Janus ultrathin films decorated with superhydrophobic and hydrophilic surfaces.[19] The self-assembly strategy at the air–water interface is considered to be an effective and robust way to fabricate a Janus film.[20–24] However, in spite of the self-assembled Janus films being successfully acquired, their designability, controllability and expansibility are still challenging.

Since an interface such as the air–liquid interface and the liquid–liquid interface can further behave as an active platform for asymmetric physical or chemical reactions, a series of Janus materials are exquisitely designed to realize multi-functionality for various applications.[25–30] Recently, Zhang *et al.* creatively introduced the concept of supramolecular interfacial polymerization for fabricating functional polymeric materials at the water–oil interface.[31] More recently, Wang *et al.* reported a one step interfacial copolymerization strategy to achieve a monolithic hydro/organo macro copolymer using hydrophobic and hydrophilic monomers.[32] The novel interfacial asymmetric modification method provides a powerful pathway for designing Janus films with well-controlled functionality.

As a typical and marvellous interfacial Janus material, the lotus leaf exhibits superhydrophobic and superhydrophilic properties at the upper and lower surfaces, respectively.[29,33] Inspired by the integrated system of the lotus leaf, herein, we describe an interfacial self-assembly and *in situ* asymmetric modification strategy for designing well-controlled Janus hybrid films. Through a Marangoni induced self-assembly and a subsequent aging process, a hydrophilic group modified carbon nanotube (CNT) film with asymmetric wettability could be readily achieved at the air–water interface.[34] In contrast, some strategies including filtration,[35] doctor blading,[36] spray-coating,[37] *etc.*[38] usually attached onto the rigid targets without desirable transferability. More importantly, when exposed to an interface with differentiated features, these achieved films with symmetric wettability or functionality cannot maintain a stable state for further asymmetric decoration. Since the anisotropic film can exist stably at the air–water interface, it can further be employed as a functional platform for further asymmetric modification. In our system, oil-soluble and water-soluble molecules were applied to the air and water side of the CNT film to conduct an *in situ* asymmetric reaction for a Janus hybrid film, demonstrating potential applications in chemical sensors,[34] oil/water separation,[2,15] and solar distillation,[39] *etc.*[2,3]

The strategy for fabricating the Janus hybrid film starting from the self-assembly of carbon nanotubes (CNTs) at the air/water interface is schematically illustrated in Fig. 1. When the CNT (with hydrophilic groups) dispersion was dropped onto the water surface, the CNTs were rapidly pushed outward

[a] *Key Laboratory of Marine Materials and Related Technologies, Zhejiang Key Laboratory of Marine Materials and Protective Technologies, Ningbo Institute of Materials Technology and Engineering, Chinese Academy of Sciences, Ningbo 315201, China. E-mail: tao.chen@nimte.ac.cn, yjhuang@nimte.ac.cn, xiaopeng@nimte.ac.cn*
[b] *University of Chinese Academy of Sciences, 19A Yuquan Road, Beijing 100049, China*
[c] *Department of Chemical Engineering, National Chung Hsing University, 250 Kuo Kuang Road, Taichung 402, Taiwan*

† Electronic supplementary information (ESI) available. See DOI: 10.1039/c8cc07143h

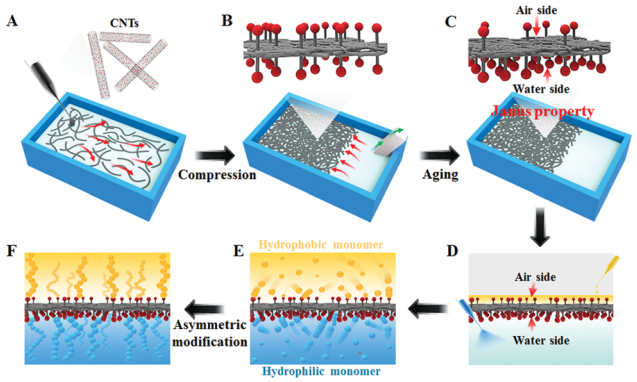

Fig. 1 Schematic illustration of the interfacial self-assembly of the CNT film and interfacial asymmetry modification of the Janus hybrid film. (A) Dropping ethanol dispersions onto the surface of water. (B) A closely packed film was achieved using a capillary force driven compression strategy. (C) The resulting CNT film demonstrated asymmetric wettability *via* a controlled aging procedure. (D) Hydrophobic and hydrophilic monomers were individually added to the air side and the water side of the CNT film for asymmetric modification. (E and F) A Janus hybrid was acquired through an interfacial asymmetric reaction.

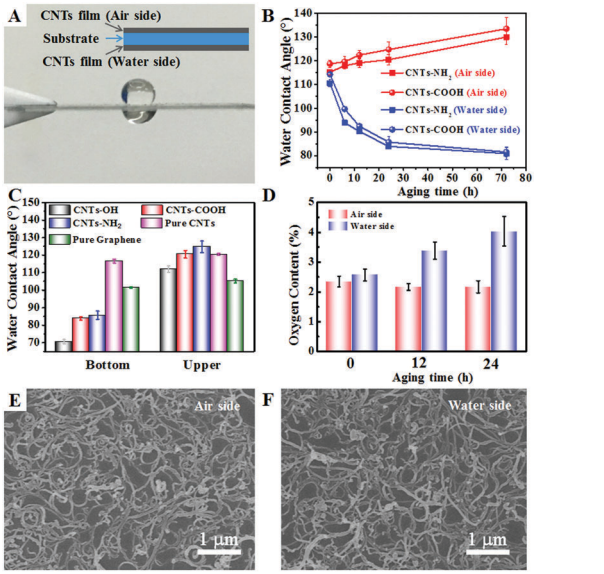

Fig. 2 (A) Photograph of the water drops at the different sides of the CNT film with –COOH groups. (B) Water contact angle (WCA) for both sides of CNT films with –COOH and NH_2 groups with different aging times. (C) WCA for both sides of a series of carbon-based films with 72 h of aging time. (D) Oxygen content measurements for both sides of the CNT film with –COOH groups at different aging times. SEM images of the CNT film of the air side (E) and the water side (F).

from ethanol-rich regions with low surface tension to water-rich regions with high surface tension owing to the strong Marangoni force (Fig. 1A).[34] Subsequently, a homogenously pre-assembled CNT layer was formed on the water surface. When a porous sponge was put on one side of the film surface, it experienced a rapid compression process from a loosely compacted state to a closely packed one (Fig. 1B). After a specific aging procedure, the CNT film with asymmetric wettability was self-assembled. Note that there were more hydrophilic groups (such as –COOH, NH_2 and –OH) on the water side than on the air side (Fig. 1C). Furthermore, contributing to the Janus wettability of the film, it could be employed as a functional platform for an asymmetric interfacial reaction. As displayed in Fig. 1D, hydrophobic and hydrophilic substances were simultaneously added to the top and bottom layer of the CNT film. As a result, a Janus hybrid film was finally achieved, in which hydrophobic and hydrophilic groups were modified on the air side and the water side of the CNT film, respectively (Fig. 1E and F).

The example of the CNT film with –COOH groups strongly shows the difference of the wettability between the air side and the water side (Fig. 2A), in which each side of the aged film was transferred to the same glass substrate. To investigate the self-assembly process, water contact angle (WCA) measurements were conducted to explore the WCA change during the aging procedure. As shown in Fig. 2B, with the increase of aging time, the WCA of the air side of the CNT film exhibited a gradual increase ranging from $\sim 115^\circ$ to $\sim 130^\circ$. Nevertheless, the WCA of the water side demonstrated a remarkable decrease from $\sim 110^\circ$ to $\sim 80^\circ$. It is noted that the self-assembly behaviour is time-dependent and can happen to some hydrophilic groups. When the $-NH_2$ and –OH functionalized CNTs were adopted to fabricate the film at the air/water interface, it can be observed that the WCA can present a similar trend (Fig. 2C).

Note that surface morphology and chemical groups can both affect the wettability of the surface. To further explore the potential self-assembly mechanism which dominates the surface wettability, pure CNTs were introduced into this system. As displayed in Fig. 2C, both sides of the pure CNT film demonstrated similar WCAs with the increase of aging time. This result indirectly evidences that the chemical groups dominate the self-assembly process. In addition, the pure graphene film also exhibits the same phenomenon. Moreover, energy dispersive spectroscopy (EDS) was used to investigate the group content of both sides of the film. Fig. 2D indicates that the oxygen content of the CNT film with –COOH groups at the water side experiences a gradual increase with the increase of aging time. Owing to the limited depth of penetration of electrons, the content on the air side just has a slight decrease, which can also verify the above-mentioned self-assembly mechanism. Furthermore, the morphology information of the CNT film was characterized by SEM measurements. As shown in Fig. 2E and F, there was no prominent structural difference observed in the morphology of the CNT film on each side.

To further investigate the asymmetric wettability of different sides of the film, the CNT–OH film was taken as an example for further experiments. As shown in Fig. S1A (ESI†), a hydrophobic substrate (WCA of $\sim 140^\circ$) was employed to transfer the CNT film at the air–water interface from the air and water side, respectively. Compared with the apparent breakage of the film transferred from the water side, the film acquired from the air side represented an integrated morphology. On the contrary, the superhydrophilic substrate (WCA of $\sim 6^\circ$) allows the film to have an intact transfer from the water side and results in failed transfer from the air side (Fig. S1B, ESI†). Upon increasing the WCA value of the substrate up to $\sim 60^\circ$, it can be observed that

the air side of the film still cannot maintain a stable state (Fig. S1C, ESI†). Significantly, the substrate with an appropriate wettability (such as the WCA of ~108°) enabled successful transfer no matter whether from the air side or the water side, ensuring the specific application in further characterization and modification (Fig. S1D and Movie 1, ESI†). The results strongly evidenced the asymmetric wettability of the as-prepared CNT film assembled at the air–water interface.

In addition to the air–liquid interface, the stability of the CNT film at the liquid–liquid interface, especially the oil–water interface, was also explored in our system before aging and after 72 h of aging time. Fig. S2 (ESI†) demonstrated that a series of organic solvents that were lighter than water (*N*-heptane, toluene, liquid paraffin, petroleum ether, ethyl acetate) were added onto the air side of the aged CNT–OH film floating on the water surface. The result shows that the CNT film can maintain a stable state after 16 hours or even longer. Nevertheless, when octanol, *N*-hexanol and cyclohexanone were added to the system, the CNT film experienced an irreversible breakage. In order to illustrate the possible mechanism, the physical properties of these organic solvents were investigated. From Table S1 (ESI†), it could be observed that organic solvents that dissolve more water would severely affect the stability of the film at the oil–water interface. In comparison, there is no prominent relation with the surface tension or the solubility in water of organic solvents. It is noted that detailed experiments will be conducted to have a better understanding of the mechanism in further work. Furthermore, ethyl acetate was selected to investigate the stability of the CNT film at the oil/water interface before and after the aging procedure. As shown in Fig. S3 (ESI†), compared with the CNT film without an aging procedure, the aged one maintains a more stable state, indicating that the aging process can remarkably enhance the stability of the resulting film.

Since the as-prepared CNT film demonstrates asymmetric wettability and excellent stability at a specific oil–water interface, it could further be employed as a functional platform for a specific reaction (Fig. 3A). As a proof of concept, 1*H*,1*H*,2*H*,2*H*-perfluorodecyltriethoxysilane (PFDTS) in heptane and dopamine in Tris solution were added onto the air and water side of the CNT (–OH group) film, which results in a stable state at the oil–water interface without any breakage (Fig. 3B). Through a typical dehydration reaction, PFDTS could be chemically modified on the CNT surface.[35,40] Whereas, the self-polymerized polydopamine (PDA) can form a strong π–π stacking interaction and multi-hydrogen bonding with CNTs.[41,42] After an appropriate reaction time, an integrated and stable Janus hybrid film was achieved in Fig. 3C. Furthermore, SEM measurements were conducted to characterize the surface morphology of the asymmetrically modified CNT film. As displayed in Fig. 3D, the hydrophobic PFDTS modified CNT layer demonstrates that the nanotubes were covered by thin layers with remarkable network structures. The result shows that the rough structure of the CNT film was commendably maintained. In comparison, the PDA modified layer was thicker than that of the PFDTS, resulting in a thickened tubular structure (Fig. 3E). Fig. 3F–I illustrate the cross-sectional information of the resulting 2D

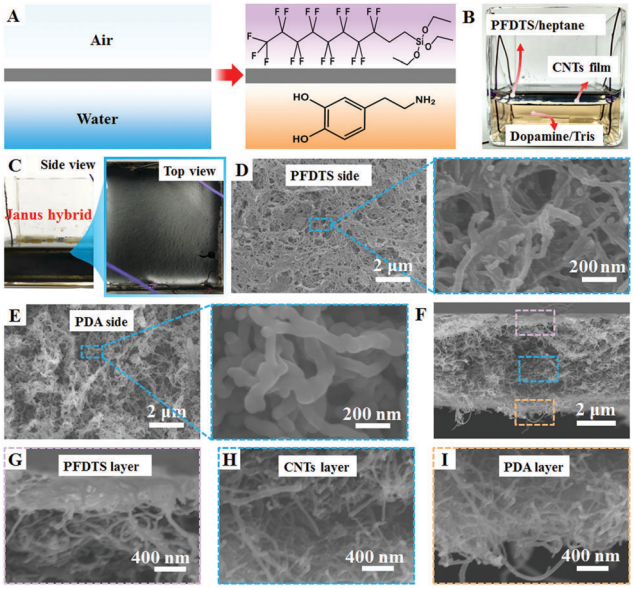

Fig. 3 (A) Schematic illustration of the interfacial asymmetric modification of the CNT film. (B) Photo of the PFDTS-heptane solution and dopamine Tris solution added to the air side and water side of the CNT film for asymmetric modification. (C) The resulting 2D Janus hybrid film after 12 h of reaction. (D) SEM images of the PFDTS modified CNT film on the air side and (E) PDA modified CNT film at the water side. (F–I) Cross-sectional images of the 2D Janus hybrid film.

Janus hybrid film and represent a remarkable sandwiched microstructure. The successful modification strongly evidenced the feasibility of the interfacial asymmetric modification strategy.

Moreover, the chemical component of the resulting Janus hybrid film was also explored through X-ray photo-electron spectroscopy (XPS) analysis. As shown in Fig. 4A, after 72 h of aging time, there were three signals at 284.4 eV (graphite), 284.8 eV (sp^3), and 286.6 eV (C–O) in the spectra of both sides of the CNT (–OH group) films, which is consistent with the reports in the literature.[43] It was observed that the oxygen content on the water side (atomic concentration, 7.38%) is higher than that on the air side (atomic concentration, 5.96%), which was consistent with the EDS measurements. After an interfacial asymmetric reaction, the PDA and PFDTS modified layers present prominent N 1s and F 1s peaks, respectively. There were six signals at 284.4 eV (C–C), 285.6 eV (C–N), 286.6 eV (C–O), 288.0 eV (C═O), 291.8 eV ($–CF_2–$) and 294.0 eV ($–CF_3$) for PDA and PFDTS modified CNT films. Attributed to the porous network of the resulting Janus hybrid film (Fig. S3, ESI†), the PDA side and the PFDTS side also demonstrate weak F 1s and N 1s peaks, respectively. However, compared with the strong N 1s or F 1s peak, the corresponding content is extremely low, which will not impact the wettability of each side of the film (Table S2, ESI†).

For adjusting the reaction time of dopamine, the self-polymerized PDA can remarkably enhance the strength of the resulting CNT hybrid film. As displayed in Fig. 4B, a self-supported Janus hybrid film was successfully acquired and presented different surface morphologies on each side of the film. Compared with the smooth layer of the PDA side, the PFDTS modified one

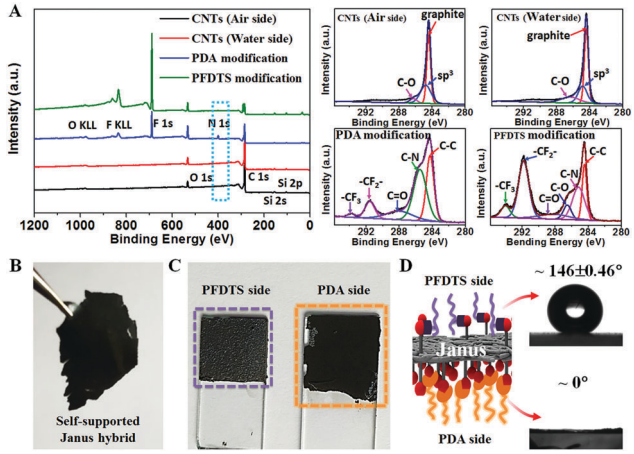

Fig. 4 (A) XPS spectra of both sides of the original CNT films and asymmetrically modified CNT films and corresponding C 1s XPS spectra. (B) Photograph of the as-prepared self-supported Janus hybrid film. (C) Photo of different sides of the Janus hybrid film. (D) WCA of different sides of the 2D Janus hybrid film.

represented a relatively rough surface due to the thinner encapsulation of PFDTS, which was consistent with the SEM images (Fig. 4C). Attributed to the successful and efficient modification of the hydrophobic and hydrophilic groups, the as-prepared Janus hybrid film demonstrates asymmetric wettability on the air and water side, resulting in $\sim 146 \pm 0.46^{\circ}$ and $\sim 0^{\circ}$, respectively (Fig. 4D).

In conclusion, we develop an interfacial self-assembly and asymmetric modification strategy for constructing a 2D Janus hybrid film at the air/water and oil/water interface. Through a Marangoni induced self-assembly with a subsequent aging procedure, a CNT film with asymmetric wettability could be readily achieved. Furthermore, as a functional reaction platform, the resulting CNT film can be simultaneously modified with hydrophobic and hydrophilic groups at the air and water side, respectively. The achieved 2D Janus hybrid film shows asymmetric structure and wettability properties, which provides an alternative approach to construct a Janus film and demonstrates significant potential in sensors, oil/water separation and solar distillation, *etc.*

This study was supported by the Natural Science Foundation of China (51803226 and 51573203), the Key Research Program of Frontier Sciences, the Chinese Academy of Sciences (QYZDB-SSW-SLH036), the Postdoctoral Innovation Talent Support Program (BX20180321), the China Postdoctoral Science Foundation (2018M630695), the Youth Innovation Promotion Association of Chinese Academy of Science (2016268 and 2017337) and the Ningbo Science and Technology Bureau (2018A610108).

Conflicts of interest

There are no conflicts to declare.

Notes and references

1 F. Liang, B. Liu, Z. Cao and Z. Yang, *Langmuir*, 2018, **34**, 4123–4131.
2 H. C. Yang, J. Hou, V. Chen and Z. K. Xu, *Angew. Chem., Int. Ed.*, 2016, **55**, 13398–13407.
3 A. Walther and A. H. Muller, *Chem. Rev.*, 2013, **113**, 5194–5261.
4 J. Hu, S. Zhou, Y. Sun, X. Fang and L. Wu, *Chem. Soc. Rev.*, 2012, **41**, 4356–4378.
5 X. Pang, C. Wan, M. Wang and Z. Lin, *Angew. Chem., Int. Ed.*, 2014, **53**, 5524–5538.
6 A. Walther and A. H. E. Müller, *Soft Matter*, 2008, **4**, 663–668.
7 M. Lattuada and T. A. Hatton, *Nano Today*, 2011, **6**, 286–308.
8 S. Jiang, Q. Chen, M. Tripathy, E. Luijten, K. S. Schweizer and S. Granick, *Adv. Mater.*, 2010, **22**, 1060–1071.
9 A. H. Groschel, A. Walther, T. I. Lobling, J. Schmelz, A. Hanisch, H. Schmalz and A. H. Muller, *J. Am. Chem. Soc.*, 2012, **134**, 13850–13860.
10 A. P. Zakharov and L. M. Pismen, *Soft Matter*, 2018, **14**, 676–680.
11 G. Chen, Y. Xu, D. G. Yu, D. F. Zhang, N. P. Chatterton and K. N. White, *Chem. Commun.*, 2015, **51**, 4623–4626.
12 A. A. Shah, B. Schultz, W. Zhang, S. C. Glotzer and M. J. Solomon, *Nat. Mater.*, 2015, **14**, 117–124.
13 H.-C. Yang, W. Zhong, J. Hou, V. Chen and Z.-K. Xu, *J. Membr. Sci.*, 2017, **523**, 1–7.
14 S.-W. Ng, N. Noor and Z. Zheng, *NPG Asia Mater.*, 2018, **10**, 217–237.
15 J. Gu, P. Xiao, J. Chen, J. Zhang, Y. Huang and T. Chen, *ACS Appl. Mater. Interfaces*, 2014, **6**, 16204–16209.
16 P. Xiao, C. Wan, J. Gu, Z. Liu, Y. Men, Y. Huang, J. Zhang, L. Zhu and T. Chen, *Adv. Funct. Mater.*, 2015, **25**, 2428–2435.
17 A. Walther, X. Andre, M. Drechsler, V. Abetz and A. H. E. Müller, *J. Am. Chem. Soc.*, 2007, **129**, 6187–6198.
18 F. Liang, K. Shen, X. Qu, C. Zhang, Q. Wang, J. Li, J. Liu and Z. Yang, *Angew. Chem., Int. Ed.*, 2011, **50**, 2379–2382.
19 H. Zhang, R. Hao, J. K. Jackson, M. Chiao and H. Yu, *Chem. Commun.*, 2014, **50**, 14843–14846.
20 B. P. Binks and P. D. I. Fletcher, *Langmuir*, 2001, **17**, 4708–4710.
21 B. Liu, W. Wei, X. Qu and Z. Yang, *Angew. Chem., Int. Ed.*, 2008, **47**, 3973–3975.
22 S. G. Booth and R. A. W. Dryfe, *J. Phys. Chem. C*, 2015, **119**, 23295–23309.
23 X. C. Luu and A. Striolo, *J. Phys. Chem. B*, 2014, **118**, 13737–13743.
24 R. Deng, H. Li, J. Zhu, B. Li, F. Liang, F. Jia, X. Qu and Z. Yang, *Macromolecules*, 2016, **49**, 1362–1368.
25 H.-C. Yang, J. Hou, L.-S. Wan, V. Chen and Z.-K. Xu, *Adv. Mater. Interfaces*, 2016, **3**, 1500774.
26 X. Yang, Z. Wang and L. Shao, *J. Membr. Sci.*, 2018, **549**, 67–74.
27 M. B. Wu, H. C. Yang, J. J. Wang, G. P. Wu and Z. K. Xu, *ACS Appl. Mater. Interfaces*, 2017, **9**, 5062–5066.
28 B. G. Im, M. Do, Y. Kim, M. Cho and J. H. Jang, *ACS Appl. Mater. Interfaces*, 2018, **10**, 7602–7613.
29 Y. Zhao, C. Yu, H. Lan, M. Cao and L. Jiang, *Adv. Funct. Mater.*, 2017, **27**, 1701466.
30 H. B. Sebastian, R. M. Mayall, V. I. Birss and S. Bryant, *Langmuir*, 2017, **33**, 10125–10133.
31 B. Qin, S. Zhang, Q. Song, Z. Huang, J. F. Xu and X. Zhang, *Angew. Chem., Int. Ed.*, 2017, **56**, 7639–7643.
32 F. Zhang, J. Fan, P. Zhang, M. Liu, J. Meng, L. Jiang and S. Wang, *NPG Asia Mater.*, 2017, **9**, e380–e387.
33 Q. Cheng, M. Li, Y. Zheng, B. Su, S. Wang and L. Jiang, *Soft Matter*, 2011, **7**, 5948–5951.
34 P. Xiao, J. Gu, C. Wan, S. Wang, J. He, J. Zhang, Y. Huang, S.-W. Kuo and T. Chen, *Chem. Mater.*, 2016, **28**, 7125–7133.
35 J. Gu, P. Xiao, Y. Huang, J. Zhang and T. Chen, *J. Mater. Chem. A*, 2015, **3**, 4124–4128.
36 J. Krantz, M. Richter, S. Spallek, E. Spiecker and C. J. Brabec, *Adv. Funct. Mater.*, 2011, **21**, 4784–4787.
37 Z. Liu, K. Parvez, R. Li, R. Dong, X. Feng and K. Mullen, *Adv. Mater.*, 2015, **27**, 669–675.
38 J. Yang, M. K. Choi, D. H. Kim and T. Hyeon, *Adv. Mater.*, 2016, **28**, 1176–1207.
39 H. Ghasemi, G. Ni, A. M. Marconnet, J. Loomis, S. Yerci, N. Miljkovic and G. Chen, *Nat. Commun.*, 2014, **5**, 4449–4455.
40 M. Jin, J. Wang, X. Yao, M. Liao, Y. Zhao and L. Jiang, *Adv. Mater.*, 2011, **23**, 2861–2864.
41 S. Wan and Q. Cheng, *Adv. Funct. Mater.*, 2017, **27**, 1703459.
42 L. Q. Xu, W. J. Yang, K.-G. Neoh, E.-T. Kang and G. D. Fu, *Macromolecules*, 2010, **43**, 8336–8339.
43 L. Wang, J. Zhao, S. Bai, H. Zhao and Z. Zhu, *Chem. Eng. J.*, 2014, **254**, 399–409.